Self-Reaction of HO_2 and DO_2: Negative Temperature Dependence and Pressure Effects

MICHAEL MOZURKEWICH* and SIDNEY W. BENSON
The Loker Hydrocarbon Research Institute, University of Southern California, University Park MC 1661, Los Angeles, California 90089

Abstract

The negative temperature dependence, pressure dependence, and isotope effects of the self-reaction of HO_2 are modeled, using RRKM theory, by assuming that the reaction proceeds via a cyclic, hydrogen-bonded intermediate. The negative temperature dependence is due to a tight transition state, with a negative threshold energy relative to reactants, for decomposition of the intermediate to products. A symmetric structure for this transition state reproduces the observed isotope effect. The weak pressure dependence for DO_2 self-reaction is due to the approach to the high-pressure limit. Addition of a polar collision partner, such as ammonia or water vapor, enhances the rate by forming an adduct that reacts to produce deexcited intermediate. A detailed model is presented to fit the data for these effects. Large ammonia concentrations should make it possible to reach the high-pressure limit of the self-reaction of HO_2.

I. Introduction

The self-reaction of hydroperoxy radical,

$$HO_2 + HO_2 \longrightarrow H_2O_2 + O_2$$

is an important atmospheric sink for odd hydrogen as well as the principal source of H_2O_2 in the stratosphere. This reaction exhibits a number of interesting features that have significance for determining the rate constant under atmospheric conditions [1]. These include a pronounced negative activation energy of -1.2 kcal mol^{-1} [2–5], a definite pressure dependence [6,7], and an enhancement of the rate constant by small amounts of water vapor [8,9]. The addition of small amounts of NH_3 initially enhances but then suppresses the reaction [9,10]. The self-reaction of DO_2 shows similar behavior but with a smaller rate constant [9] and a weaker pressure dependence [2].

It has been proposed [1,5] that the negative activation energy and the pressure dependence are due to the formation of a dimer

$$HO_2 + HO_2 \rightleftharpoons (HO_2)_2^* \longrightarrow H_2O_2 + O_2$$

and that the water vapor and ammonia enhancements are due to complex formation [9]

$$HO_2 + H_2O \rightleftharpoons HO_2 \cdot H_2O$$

with the subsequent reaction

$$HO_2 \cdot H_2O + HO_2 \longrightarrow H_2O_2 + O_2 + H_2O$$

being much faster than the reaction of uncomplexed HO_2. In Section II we present a modified mechanism for this behavior.

Patrick, Barker, and Golden [11] have carried out calculations of the rate constant making the assumption that the intermediate is a tetraoxide, HOOOOH. In order to fit the data they needed to make some extreme assumptions about the properties of the intermediate. As explained below, we think that this model does not adequately explain either the isotope or water vapor effects.

Kircher and Sander [2] have also carried out RRKM calculations assuming a tetraoxide intermediate. Like Patrick, Barker, and Golden they find that fitting the pressure dependence requires that the intermediate be either unreasonably strongly bound or extremely loose. They present no calculations for either the water vapor or isotope effects.

It has also been proposed [5,12] that the intermediate is a cyclic, hydrogen-bonded dimer, Figure 1. Because of the difficulties with the tetraoxide model, we have also assumed that the intermediate has this cyclic structure. In Section III we describe the assignment of parameters for this intermediate and the transition state. The results of calculations of the temperature and pressure dependence of the rate constants are presented in Section IV. These calculations use the method presented previously [13]. In Section V we present results for

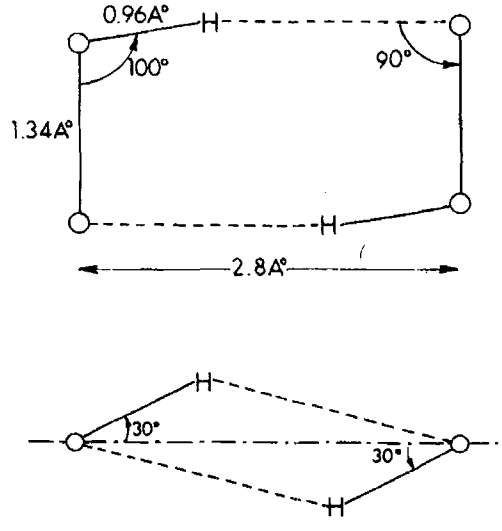

Figure 1. Geometry of proposed intermediate.

the water vapor and ammonia effects. Finally, we summarize our conclusions and suggest ways in which experiments might test the proposed model.

II. Reaction Mechanism and Rate Expressions

We assume that the reaction proceeds via an excited dimer:

(1) $$HO_2 + HO_2 \rightleftharpoons (HO_2)_2^{**}$$

The forward reaction proceeds at essentially collision frequency, much faster than the experimental rate constant. Thus, this reaction will be in equilibrium.

The dimer may decompose to products (essentially all hydrogen peroxide and O_2) [14],

(2) $$(HO_2)_2^{**} \longrightarrow H_2O_2 + O_2$$

or undergo collisional stabilization,

(3) $$(HO_2)_2^{**} + M \rightleftharpoons (HO_2)_2^{*} + M$$

to a less excited state.

We assume that the potential energy surface is like that in Figure 2, so that the barrier for decomposition to products is lower than for decomposition to reactants. Hence, the less excited dimer can go directly to products

(4) $$(HO_2)_2^{*} \longrightarrow H_2O_2 + O_2$$

In the presence of water vapor (or ammonia), we may form a hydrogen-bonded hydrate [9,15]

(5) $$HO_2 + H_2O \rightleftharpoons HO_2 \cdot H_2O$$

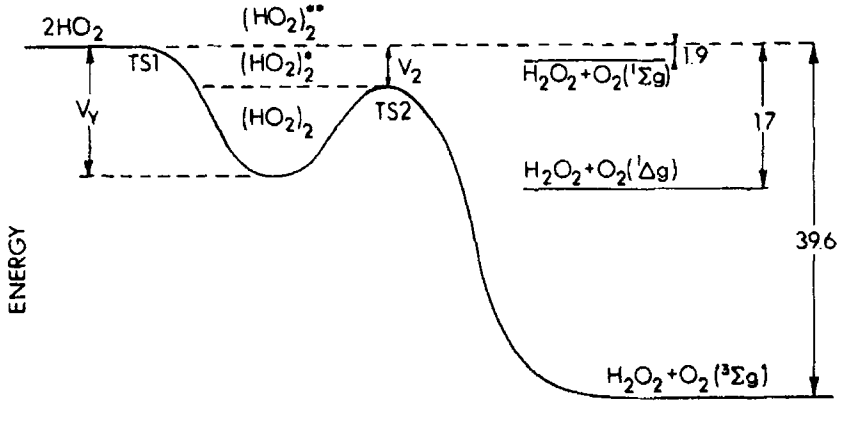

Figure 2. Schematic potential energy surface for a reaction proceeding through an intermediate. The ground state of the reactants is taken as the zero of energy. Energies are in kcal mol^{-1}.

The lifetime of the hydrate with respect to unimolecular decomposition is, for a 7 kcal mol^{-1} hydrogen bond, about $10^{-13} \exp(E/RT) = 10^{-8}$ s in the high-pressure limit and about $[(10^{19}$ molecules $cm^{-3}) \cdot (10^{-11}$ cm^3 molecules^{-1} $s^{-1})]^{-1} \exp(E/RT)Q/N(E) \ll 10^{-3}$ s in the second-order limit [Q is the partition function and $N(E)$ is the density of states at threshold]. Therefore, this lifetime is small compared to the millisecond experimental time scale and reaction (5) will be in equilibrium.

HO_2 may displace the water molecule to form the stabilized dimer [1] in an exothermic reaction:

$$HO_2 + HO_2 \cdot H_2O \rightleftharpoons (HO_2)_2 + H_2O \tag{6}$$

The reaction lifetime of the hydrate is $([HO_2]k_6)^{-1} > 10^{-14}$ $10^{10} = 10^{-4}$ s so reaction (6) will not significantly perturb the equilibrium of reaction (5).

The stabilized dimer may undergo collisional excitation

$$(HO_2)_2 + M \rightleftharpoons (HO_2)_2^* + M \tag{7}$$

followed by reaction (4). As long as reaction (7) is in steady state, it will have no effect on the rate in the absence of water vapor.

Since reactions (3), (4), and (7) involve species which are in steady state, rather than in equilibrium, the rate constants depend on the form of the nonthermal distribution function. Since data for the water vapor effect, or in the fall-off region, are sparse, we do not attempt to rigorously account for this. Instead, we treat the rate constants as having their thermal values.

In Figure 3 we show two possible structures for the hydrate. Hamilton and Naleway [16] have argued in favor of structure (b). We prefer structure (a), in which the hydrogen bond involves the half-filled orbital in HO_2. In either structure the water molecule should interfere with the head-to-tail interaction required to form the hydrogen-bonded dimer. Hence, we assume that the reaction

$$HO_2 \cdot H_2O + HO_2 \cdot H_2O \longrightarrow \text{products}$$

does not take place.

The above mechanism encounters difficulties if the dimer has the tetraoxide structure. As we shall see below, the displacement, reaction (6), must proceed at essentially collision frequency (10^{-10} cm^3 molecules^{-1} s^{-1}). If the hydrate has the structure shown in Figure 3(a), we would expect the water molecule to interfere with the formation of the tetraoxide. In fact, for the addition of HO_2 to $HO_2 \cdot H_2O$, k_6 is apparently a factor of 5 or more smaller than for HO_2 self-reaction [17]. However, if the hydrate has structure (b), there is no reason why the hydrate self-reaction should not be very rapid. This makes it difficult to understand the reduction in rate at large ammonia concentrations [9].

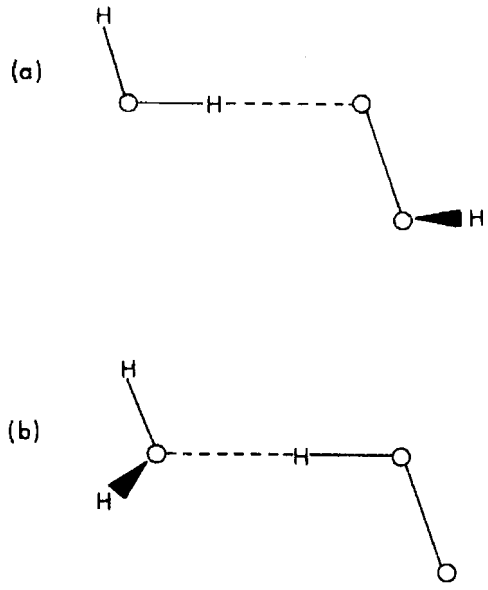

Figure 3. Proposed structures for the HO_2 hydrate.

In the following, we use k to designate a rate constant and K for an equilibrium constant. At low pressure, the apparent bimolecular rate constant, k_{II} is

$$k_{II} = k_2 K_1 \tag{8}$$

and the termolecular rate constant, k_{III} is

$$k_{III} = k_3 K_1 \tag{9}$$

Assuming that the dimer is in thermal equilibrium with the reactants, we obtain the high-pressure limit, k_∞, as

$$k_\infty = (k_2 + k_4 K_3) K_1 \tag{10}$$

In the absence of water vapor the experimental rate constant is

$$k_{exp} = (k_2[(HO_2)_2^{**}] + k_4[(HO_2)_2^{*}])/[HO_2]^2$$

Assuming that the highly excited dimer is in equilibrium and the less excited dimer is in steady state, we obtain

$$k_{exp} = k_2 K_1 + \{k_4 k_3 [M] K_1/(k_4 + k_{-3}[M])\}$$

Using eqs. (8) to (10), this becomes

$$k_{exp} = k_{II} + \{k_{III}[M]/[1 + k_{III}[M]/(k_\infty - k_{II})]\} \tag{11}$$

This Lindemann-type fall-off curve implicitly assumes that the less excited dimer is described by an equilibrium distribution function. This approximation will have little effect since all of the experimental data are either near the low-pressure, linear region or are at temperatures at which k_{II} and k_∞ are not too different.

In the presence of H_2O (or NH_3), the experimental rate constant is given by

(12) $$k_{exp} = \{k_2[(HO_2)_2^{**}] + k_4[(HO_2)_2^*]\}/\{[HO_2](1 + K_5[H_2O])\}^2$$

We again assume that reaction (1) is in equilibrium and that the less excited and deexcited dimer are in steady state. From these latter conditions, we obtain

(13) $$\frac{[(HO_2)_2^*]}{K_{eq}^*[HO_2]^2} = \frac{k_6K_5[H_2O] + k_{III}[M]/f}{k_6K_5[H_2O] + (k_{III}[M] + k_\infty - k_{II})/f}$$

where

$$K_{eq}^* = K_1K_3 = K_5K_6K_7$$

and

(14) $$f = \frac{k_{-7}[M]K_{eq}^*}{k_{-7}[M]K_{eq}^* + k_6K_5[H_2O]}$$

Substituting (13) into (12), we obtain

(15)

$$k_{exp} = k_{II} + \frac{k_{III}[M] + fk_6K_5[H_2O]}{1 + (k_{III}[M] + fk_6K_5[H_2O])/(k_\infty - k_{II})} \Big/ (1 + K_5[H_2O])^2$$

Equation (15) is very similar to that for the fall-off curve, eq. (11). The rate of forming stabilized dimer via the hydrate is now added to the collisional deexcitation term. The denominator in (15) accounts for the reduction in free HO_2 due to hydrate formation.

Using the definition of K_{eq}^*, we may rewrite eq. (14) as

(16) $$f = k_7[M]/(k_7[M] + k_{-6}[H_2O])$$

Since the stabilized intermediate sometimes undergoes back-reaction with H_2O rather than collisional dissociation, f might be less than 1. This will reduce the water vapor effect; we expect this to occur at sufficiently low pressures [M].

Reaction (6) may be considered to occur in two consecutive stages. In the first step HO_2 forms a dipole bond to the HO_2 end of $HO_2 \cdot HOH$. This is about 7 kcal exothermic and sufficiently energetic to displace the water molecule. Alternatively the added HO_2 can displace the H_2O molecule in a step which is nearly thermoneutral. The overall reaction (6) is thus about 6 to 7 kcal exothermic. The reverse step (−6) is then about 6–7 kcal endothermic and is expected to be much slower than the competing excitation to the second transition state $(HO_2)_2^*$ forming products. The fastest step for the $(HO_2)_2$ formed by H_2O displacement [step (6)] is certainly deexcitation to ground state $(HO_2)_2$. However, this latter will most probably redissociate to products, making step (6) essentially rate determining for product formation. Thus, we may set $f = 1$ except at very high $(H_2O)/(M)$ ratios.

We can put f in a form that is easier to evaluate by assuming that the collision efficiencies are the same for deexcitation of both $(HO_2)_2^{**}$ and $(HO_2)_2^*$. Then,

$$k_{-7} = k_3 k_{III}/k_1$$

and

$$f = k_{III}[M]K_3/(K_{III}[M]K_3 + k_6 K_5[H_2O]) \tag{17}$$

From this and eq. (15), we see that when $K_3 = 0$ (i.e., $V_2 = O$), the addition of water vapor will not increase the reaction rate.

In the high-pressure limit, eq. (15) reduces to

$$k_{exp} = k_\infty/(1 + K_5[H_2O])^2 \tag{18}$$

In contrast to the situation at low pressure, water vapor reduces the high-pressure limiting rate constant by reducing the equilibrium concentration of dimer.

III. Description of Intermediate and Transition States

As noted above, previous workers [2,11], using a tetraoxide model for the intermediate, have had difficulties in explaining the experimental data. For our calculations we have adopted the cyclic structure shown in Figure 1. This dimer may be bound by as much as 15 kcal mol^{-1}. The binding energy of the tetraoxide, estimated from the tertiary butyl analog [18], is only about 9 kcal mol^{-1}. We assume that the reaction proceeds on the triplet surface only. In contrast, if the intermediate is a tetraoxide then we would expect the product O_2 to be in a singlet state.

The referees have brought a recent *ab initio* calculation [19] to our attention. This calculation gives the cyclic HO_2 dimer a planar geometry with a binding energy of only about 5 kcal mol^{-1}. Since the calculated vibrational frequencies are not in particularly good agreement with observed values, we are not sure how much credence should be given to the calculated binding energy. If V_2 (Fig. 2) is to be about -5 kcal mol^{-1} (as determined below), we must require the dimer to be bound by somewhat more than 5 kcal mol^{-1} to allow the transition state to have an activation energy relative to the intermediate.

When the dimer initially forms, we expect it to have an extended, head-to-tail, singly-hydrogen-bonded structure: $HO\dot{O}\cdots HO\dot{O}$. We can make a conservative estimate of the ring closing rate by assuming that the transition state for ring closure has the same structure as the closed ring and the same energy as the open dimer. In this case, the density of states (at an energy of about 8 kcal mol^{-1}) of the open form is about 300 times that of the transition state. At lower ener-

gies, the ratio is smaller. Thus, the lifetime for closure should be about 300 vibrational lifetimes, i.e., about 10^{-11} s. This is about what we estimate for the lifetime for dissociation of dimer to reactants. Actually, the closure lifetime should be less than this since (1) the potential energy should decrease as the ring closes, (2) the transition state should be looser than the fully closed ring, and (3) the energy may well be less than 8 kcal mol^{-1}.

Hence, of the three steps—forming the open dimer, closing the ring, and dissociating to products—the second should be fastest. As we shall see below, the first step has little effect on the overall rate constant. Therefore, it seems safe to regard the ring opening and closing as being fast and to treat the open and closed dimers as different states of a single intermediate. In calculating densities of states of the intermediate we add the densities of states of the two forms.

The overall scheme would be roughly as follows:

$$2HO_2 \underset{}{\overset{a}{\rightleftharpoons}} HOO\cdots HOO^* \overset{b}{\rightleftharpoons} \begin{matrix} O-H\cdots O^{**} \\ | \quad\quad | \\ O\cdots H-O \end{matrix}$$

with each step (a) and (b) exothermic by about 7 to 8 kcal. A small centrifugal barrier may exist in step (b), but this is more than compensated by the much larger dipole–dipole interaction. The extended dimer is estimated to have an entropy about 8 e.u. greater than the cyclic form (in their ground states). The additional excitation energy released in step (b) gives $(HO_2)^{**}$ more than enough vibrational entropy to compensate for this and make it the dominant form. For reaction (a) we estimate $\Delta S^0_{298}(a) = -27.6$ e.u. so that $\Delta S^0_a + \Delta S^0_b = -35.6$ e.u. at 298 K.

The potential energy surface for the reaction is shown in Figure 2. Due to long-range dipole–dipole interactions of the reactants, the first transition state (TS1) is very loose with no intrinsic energy barrier. We assign the fragments the same frequencies and moments of inertia as the reactants. These are presented in Table I. The assumed geometry for the reactants is $r_{OH} = 0.96$ A, $r_{OO} = 1.34$ A, $\theta_{OOH} = 100°$. In the transition state a steric factor of 1/2 is included since the dipoles must be in an attractive orientation.

TABLE I. Vibrational frequencies (cm^{-1}) and moments of inertia (amu $Å^2$) for HO_2 and DO_2.

Mode	$HO_2^{(20)}$	DO_2
OH stretch	3410	2400
HOO bend	1390	1020
OO stretch	1095	1095

HO_2 = 0.827, 15.1, 15.9.
DO_2 = 1.52, 15.8, 17.4.

TABLE II. Vibrational frequencies (cm^{-1}) and moments of inertia (amu Å) for the cyclic intermediate (see text for assignments).

Mode	Degeneracy	$(HO_2)_2$	$(DO_2)_2$
OH Stretch	2	3323	2400
HOO bend	2	1416	1000
OO stretch	2	1108	1108
	Cyclic Form		
H out of plane	2	460	340
OH—O anti-sym str.	1	435	435
OH—O sym str.	1	265	265
In plane deformation	1	160	160
Out of plane deformation	1	115	115
	Open Form		
O—HO bend	1	460	340
O—HO stretch	1	360	360
Heavy atom bending	2	100	100

Cyclic	Open
$(HO_2)_2$: 30.3, 127.0, 156.0	$(HO_2)_2$ = 19.6, 190.0, 210.0 (external)
$(DO_2)_2$: 32.0, 128.0, 158.0	$(DO_2)_2$ = 18.8, 198.0, 217.0 (external)
	1.27, 7.0 (internal)

The moments of inertia for two external rotational degrees of freedom of the transition state are determined by the separation at the top of the centripetal barrier. The first transition state affects the rate only at very low energies [20]. At these energies the centripetal barrier occurs at very large separations. Hence, we take the moment of inertia to be infinite, i.e., we assume that there is no centripetal barrier at TS1.

Six of the vibrations of the intermediate should be very similar to HO_2. Diem, Tso, and Lee [21] have observed these frequencies for the cyclic dimer; we include their values in Table II. The out-of-plane motions of the hydrogen atoms are essentially torsions with a barrier of 7 kcal mol^{-1}. There are four low-frequency vibrations associated with relative motions of the two fragments. We obtain these by modifying the corresponding frequencies of the formic acid dimer [22] using the ratios of the appropriate moments of inertia or reduced masses. For the open dimer the six low frequencies include one hydrogen out-of-plane motion, two free rotations (the terminal H about the O—O bond and the two O_2 groups about the hydrogen bond), stretching of the hydrogen bond (calculated for a Lennard-Jones potential), and two relative bending motions of the O_2 groups. The frequencies are listed in Table II. We take the bond strength to be 8 kcal mol^{-1}.

To determine the structure of the second transition state (TS2) we must first identify the reaction coordinate; this should be one of the heavy atom motions since these are slow. When the OH···O distance becomes sufficiently short, the hydrogen atom can move freely between the two oxygen atoms, as shown in Figure 4. Therefore, the re-

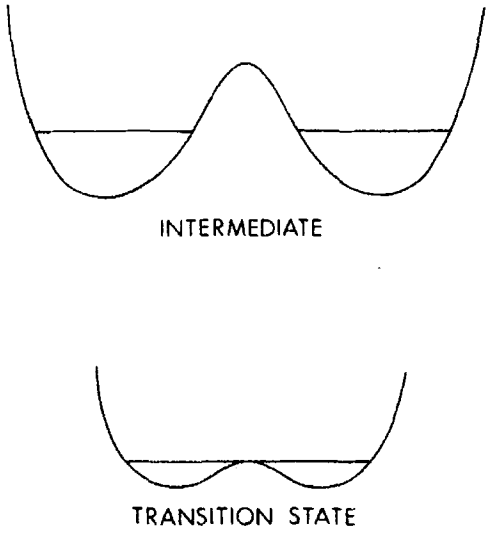

Figure 4. Potential energy surface for the ground-state hydrogen motion in the intermediate and at the transition state. As the O—O distance shortens the central barrier becomes lower.

action coordinate should be one of the OH···O stretching motions. We choose the symmetric stretch since this has a lower frequency.

This choice of reaction coordinate produces a symmetric structure for TS2 with both hydrogens moving freely between two oxygens. This structure is tighter than an asymmetrical one would be and therefore produces a more negative activation energy. Also, it gives a stronger isotope effect since both hydrogen translational motions have low frequencies.

The vibrational frequencies and moments of inertia for this transition state are listed in Table III. Referring to Figure 4 we see that the H atom moves in an essentially square well potential. For the translational motion of the H atoms we assign a frequency of 800 cm^{-1}, corresponding to the first transition for a particle in a square well 0.4 Å in length. We also have four weakened hydrogen-bending fre-

TABLE III. Vibrational frequencies (cm^{-1}) and moments of inertia (amu $Å^2$) for the second transition state.

Mode	Degeneracy	$(HO_2)_2^{\ddagger}$	$(DO_2)_2^{\ddagger}$
H translation	2	800	575
H bend	4	1000	720
O—O stretch	2	1100	1100
OH—O sym. str.	1	r.c.	r.c.
OH—O anti-sym.	1	650	650
In plane deformation	1	240	240
Out of plane twist	1	175	175

$(HO_2)_2^{\ddagger}$ = 30.1, 92.4, 122.0.
$(DO_2)_2^{\ddagger}$ = 31.6, 92.5, 123.0.

quencies of 1000 cm^{-1} [23]. The O—O stretches are intermediate between those of the products, O_2 and H_2O_2. Finally, the low-frequency modes will be somewhat stiffened since the weakest bonds between the fragments are strengthened. We have raised these frequencies, somewhat arbitrarily, by 50%.

For the self-reaction of DO_2 we have changed all frequencies in a manner consistent with the Teller-Redlich product rule [24]. The changes in zero-point energy cause V_Y (Fig. 2) to become more negative by 0.5 kcal mol^{-1} and V_2 becomes less negative by 1.5 kcal mol^{-1}

IV. Calculation of Rate Constants

We have previously [13] described a method for calculating the rate constants of reactions proceeding via excited intermediates. In the low-pressure limit this consists of the following. Once the excited intermediate is formed it may decay either to products or back to reactants. Using RRKM theory, we compute these rate constants as functions of energy and angular momentum. We can then calculate the steady-state concentration of intermediate, and therefore the rate of decay to products, as a function of E and J. These results are then integrated to obtain the total reaction rate. Obviously, the integration does not include energies below the ground state of the reactants.

If the formation of excited intermediate is very fast and the pressure is sufficiently high then the intermediate will be in thermal equilibrium with the reactants. The overall rate constants may then be calculated by applying transition state theory at TS2. This transition state theory rate constant will differ from the high-pressure limit only if it approaches the rate of formation of the excited intermediate. For the reactants considered here this latter rate will be very large, probably exceeding 10^{-10} cm^3 $molecule^{-1}$ s^{-1}. Since the experimental rate constants are much less than this, we will treat the transition state theory rate constant as the high-pressure limit.

To determine the pressure dependence of these reactions we need the low-pressure, third-order rate constant for the formation of the stabilized intermediate. We calculate this by assuming that the stabilization rate constant can be written as the product of a collision efficiency, a collision rate constant, and an equilibrium constant between the excited intermediate and the reactants. Since TS1 is very loose and the well is very shallow, we treat all external rotations as being active in calculating this equilibrium constant [13].

Calculations of k_{II} and k_∞ were carried out using the parameters listed in Tables I and IV. The properties of the intermediate have no effect on these rate constants. The value of the potential energy, V_2, at TS2 was treated as an adjustable parameter. For $HO_2 + HO_2$ the best results were achieved with $V_2 = -4.9$ kcal mol^{-1}. Appropriate zero-

TABLE IV. Calculated rate constants for low-pressure limit, k_{II}, high-pressure limit, k_∞, and low-pressure linear region, k_{III}.

Temperature (K)	$k_{II} \cdot 10^{12}$ cm^3 molec^{-1} s^{-1}	$k_\infty \cdot 10^{12}$ cm^3 molec^{-1} s^{-1}	$k_{III} \cdot 10^{32}$ cm^6 molec^{-2} s^{-1}
	$HO_2 + HO_2$		
241	3.12	248	10.5
298	1.85	30.8	6.07
417	0.874	2.86	2.57
	$DO_2 + DO_2$		
245	0.580	4.90	9.40
298	0.373	1.36	5.55
418	0.201	0.312	2.29

point energy changes then require that we use $V_2 = -3.4$ kcal mol^{-1} for $DO_2 + DO_2$. The calculated values of k_{II} and k_∞ are listed in Table IV. The large negative activation energies for k_∞ are due to the intermediate being in thermal equilibrium with the reactants.

The tetraoxide model will produce very similar results for HO_2. However, since one of the H atom frequencies of TS2 is the same as in the reactants, the zero-point energy changes will be less for this model. As a result, the isotope effect will be too weak. Patrick, Barker, and Golden [11] change V_2 by about 3 kcal mol^{-1} upon isotope substitution. However, their reported frequencies correspond to a change of only about 0.3 kcal mol^{-1}.

Also presented in Table IV are the calculated values of k_{III}. Parameters from Table II were used. The well depth for $(HO_2)_2$ was set at 15 kcal mol^{-1} for the cyclic form and 8.0 kcal mol^{-1} for the open form. For $(DO_2)_2$ we used 15.5 kcal mol^{-1} for the cyclic form and 8.3 kcal mol^{-1} for the open form. All calculations were for N_2 as the collision partner. We assumed collision radii of 1.8 Å for N_2 and 2.5 A for $(HO_2)_2$. The collision efficiency was chosen to be 0.035 in order to produce a reasonable fit to the data.

This collision efficiency is an order of magnitude smaller than usually encountered at low temperatures [25,26]. However, it is comparable to values reported near 1000 K [27,28]. Since the energy of the excited intermediate is so low in this reaction, it may be reasonable for the collision efficiency to be comparable to those measured for more energetic species at higher temperatures.

An alternate explanation is that the well depth may be much less than 15 kcal mol^{-1}. For example, weakening the hydrogen bonds by 1 kcal mol^{-1} each, we must double the collision efficiency to produce the same pressure dependence. None of the other calculations carried out here are sensitive to the well depth. Hence, we cannot determine a unique value for this parameter. Also, by treating all external rotations as being active we produce a slight overestimate of the density

of states of the intermediate. This results in a collision efficiency that is somewhat too small.

Kircher and Sander [2] have measured the rate constants for the self-reactions of HO_2 and DO_2 as functions of temperature and pressure. Their results agree well with other, less extensive, studies [3,6]. In Figures 5 and 6 we compare our calculated rate constants from eq. (11), to the measured values. The error bars shown are twice the reported standard deviations; actual 90% confidence limits should be somewhat larger due to the possibility of systematic errors.

The agreement between the calculated and experimental rate constants is excellent. The principal discrepancy is that, for $HO_2 + HO_2$, the predicted temperature dependence above 298 K is somewhat stronger than is observed. The results for $DO_2 + DO_2$ show that this reaction is in the fall-off region at pressures of a few hundred torr. As a result, the low-pressure limits are quite different, with a much weaker temperature dependence, than would be predicted by a linear extrapolation to zero pressure. Data at low temperatures, and very

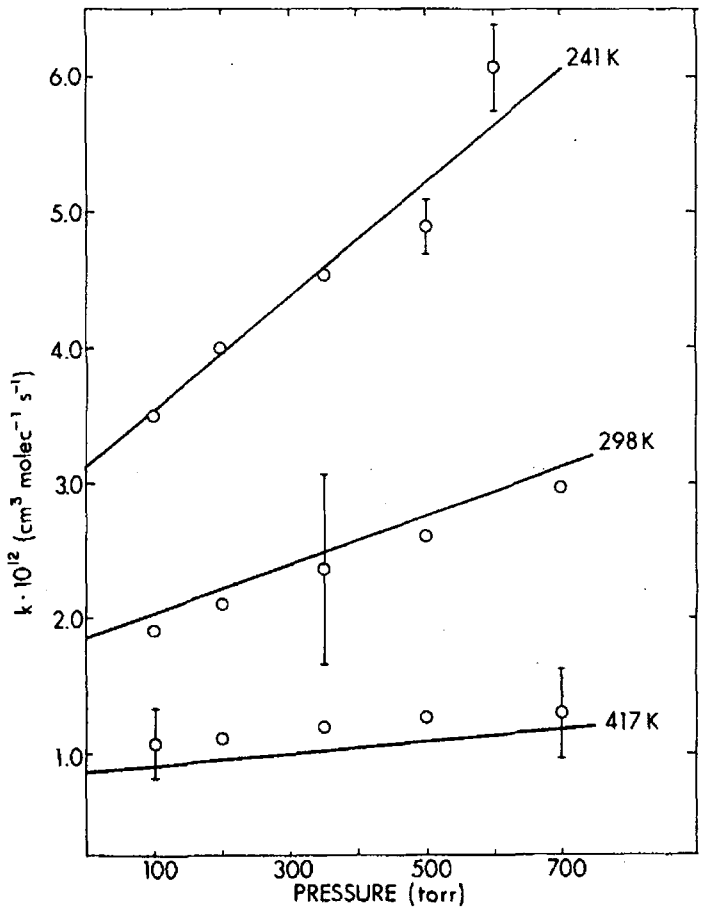

Figure 5. Comparison of calculated (solid lines) and experimental [2] (points) rate constants for $HO_2 + HO_2$. Error bars are twice the standard deviation.

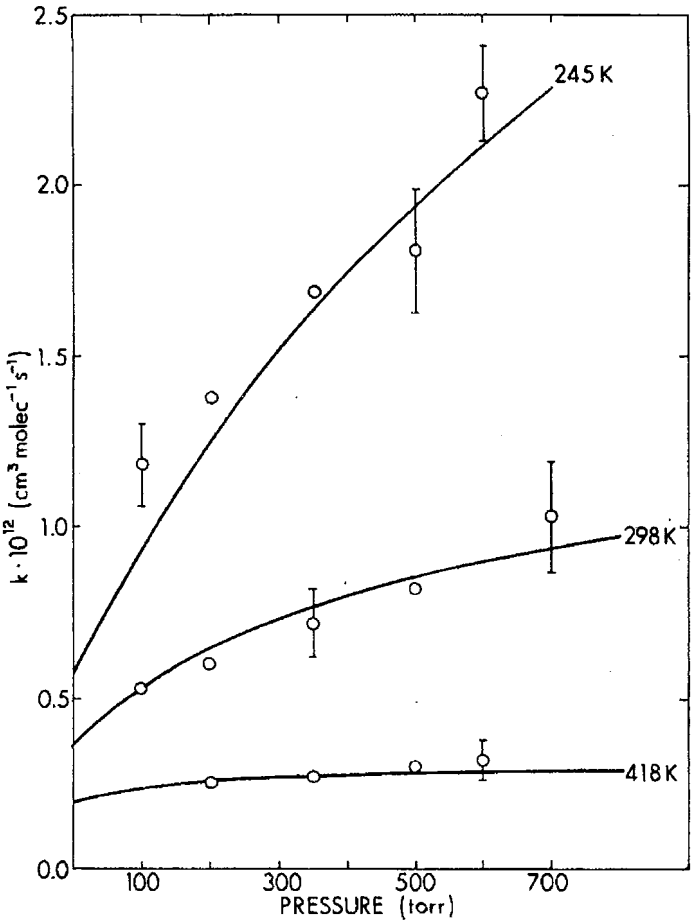

Figure 6. Comparison of calculated (solid lines) and experimental [2] (points) rate constants for DO_2 + DO_2. Error bars are twice the standard deviation.

low or very high pressures, are needed to distinguish between the linear and curved pressure dependences.

For the purpose of interpolation we have fit analytic forms to the results of our calculations. For k_{III} the temperature dependence is determined entirely by internal energy effects. Hence, a power law gives the best fit. For k_∞ an Arrhenius expression is appropriate. For k_{II} the temperature dependence is determined partly by the threshold energy, V_2, and partly by internal energy changes. For HO_2, with a more negative V_2 than DO_2, a power law gives the best fit while for DO_2 an Arrhenius expression does best. The best fits are given in Table V.

V. Rate Enhancement by Polar Species

Equation (14) gives the dependence of the experimental rate constant on the concentration of a polar adduct, such as water vapor or ammonia. Values for k_{II}, k_{III}, and k_∞ are taken from Table V. The re-

TABLE V. Expressions for the parameters needed to evaluate eq. (15).

$HO_2 + HO_2$
$k_{II} = 1.86 \cdot 10^{-12}(300/T)^{2.31}$ cm^3 molec^{-1} s^{-1}
$k_\infty = 6.26 \cdot 10^{-15} \exp(2550/T)$ cm^3 molec^{-1} s^{-1}
$k_{III} = 5.98 \cdot 10^{-32}(300/T)^{2.57}$ cm^6 molec^{-2} s^{-1}
$K_3 = 0.0268 \exp(2470/T)$
$k_6 = 1.4 \cdot 10^{-10}$ cm^3 molec^{-1} s^{-1}
for H_2O, $K_5 = 8.3 \cdot 10^{-25} \exp(3370/T)$ cm^3 molec^{-1}
for NH_3, $K_5 = 8.3 \cdot 10^{-25} \exp(3930/T)$ cm^3 molec^{-1}
$DO_2 + DO_2$
$k_{II} = 4.49 \cdot 10^{-14} \exp(628/T)$ cm^3 molec^{-1} s^{-1}
$k_\infty = 6.22 \cdot 10^{-15} \exp(1620/T)$ cm^3 molec^{-1} s^{-1}
$k_{III} = 5.49 \cdot 10^{-32}(300/T)^{2.64}$ cm^6 molec^{-2} s^{-1}
$K_3 = 0.097 \exp(1710/T)$
$k_6 = 1.4 \cdot 10^{-10}$ cm^3 molec^{-1} s^{-1}
for D_2O, $K_5 = 8.3 \cdot 10^{-25} \exp(3470/T)$ cm^3 molec^{-1}
for ND_3, $K_5 = 8.3 \cdot 10^{-25} \exp(4130/T)$ cm^3 molec^{-1}

sults of the previous section also allow us to calculate the equilibrium constant, K_3. This is given by

$$K_3 = \int_{E_1^\ddagger}^{\infty} N(E) \exp(-E/RT)\, dE \Big/ \int_{E_2^\ddagger}^{E_1^\ddagger} N(E) \exp(-E/RT)\, dE$$

where $N(E)$ is the density of states of the dimer and $E_1^\ddagger$ and $E_2^\ddagger$ are the threshold energies for decomposition to reactants and products. These are recorded in Table V.

The rate constant for the displacement of H_2O by HO_2 should be essentially collision frequency (about 10^{-10} cm^3 molecule^{-1} s^{-1} for molecules with large dipoles), and it should be independent of temperature. The exact value will be treated as an adjustable parameter.

We estimate the preexponential factor in the equilibrium constant, K_5, from the hydrate structure in Figure 3(a). We assign the hydrate a product of moments of 1.7×10^5 amu^3 A^6. The fragments are given the same frequencies as the reactants plus a free OH rotor, a hindered OH rotor (200 cm^{-1}), two bridging H atom bending motions (400 cm^{-1}), a OH$\cdots$O stretch (300 cm^{-1}), and a heavy atom bending motion (100 cm^{-1}). With these parameters we find

$$K_5 = 8.3 \times 10^{-25} \exp(V_5/RT)$$

where V_5 is the hydrogen-bond strength. We treat this as an adjustable parameter. For ammonia and for DO_2 the preexponential factor should be about the same. For DO_2 the bond strength should be 0.4 kcal mol^{-1} stronger due to zero-point energy changes.

Lii et al. have measured the temperature dependence of the rate constant of the self-reaction of water vapor [8] and ammonia [10].

These experiments were carried out in 3.8×10^{19} molecule cm^{-3} of H_2. Kircher and Sander [2] have measured the water vapor effect in 100 and 700 torr of N_2. In the absence of water vapor the data of Lii et al. are very similar to the 700 torr data of Kircher and Sander. For these two sets of data to be the same, H_2 must be 60% as effective as N_2 as a collision partner.

Ammonia has much stronger influence on the rate constant than water vapor. As a result, the ammonia effect proved to be more sensitive to the values chosen for the parameters. We therefore chose the displacement rate constant, k_6, and the hydrogen-bond strength, V_5, to fit the ammonia data. For the water vapor effect, we used the same value of k_6 and varied V_5. Reasonable fits were obtained with $k_6 = 1.4 \times 10^{-10}$ cm^3 $molecular^{-1}$ s^{-1}, $V_5(NH_3) = 7.0$ kcal mol^{-1} and $V_5(H_2O) = 6.5$ kcal mol^{-1}.

Under the experimental conditions used, no more than about 3% of the HO_2 is complexed by water vapor. As a result, we can express the water vapor effect as an apparent third-order rate constant for $HO_2 + HO_2 + H_2O$. Experimental and calculated values of this quantity are shown in Table VI. The experimental values are probably not very accurate at low temperatures, where only a small range of H_2O concentrations are available. For example, at 256 K the maximum H_2O concentration produces a rate constant only about 20% larger than in the absence of H_2O [2]; this is only a little larger than the experimental uncertainty. At higher temperatures the fit is quite good.

As noted above, in the high-pressure limit the addition of water vapor reduces the rate constant. At low pressure this tends to cause a slight negative pressure dependence. The stabilized dimer, formed via the hydrate, must as already noted, undergo collisional dissociation. The calculated rate constants (Table VI) show a negative pressure dependence at 270 K and a slight positive pressure dependence at

TABLE VI. Comparison of calculated and experimental values of the apparent third-order rate constant for $HO_2 + HO_2 + H_2O$.

Temp. (K)	Bath Gas	$[M] \cdot 10^{-19}$ molec cm^{-3}	$[H_2O]_{max} \cdot 10^{-17}$ molec cm^{-3}	Ref.	$k \cdot 10^{30}$ cm^6 $molec^{-2}$ s^{-1} exper.	calc.
256	N_2	0.38	0.295	[2]	18	38
270	N_2	2.5	0.888	[2]	17	18
270	N_2	0.36	0.883	[2]	14	19
285	N_2	0.34	3.12	[2]	7.3	8.6
298	N_2	2.3	4.41	[2]	5.8	5.03
298	N_2	0.32	4.41	[2]	3.8	4.97
298	H_2	3.8	6.5	[8]	5.9	4.7
323	H_2	3.8	15.6	[8]	1.8	1.7
348	H_2	3.8	20.5	[8]	0.83	0.73
373	H_2	3.8	22.0	[8]	0.37	0.36

298 K. The calculated value in H_2 at 298 K is small due to curvature at larger H_2O concentrations.

In Figure 7 we compare the calculated and experimental rate constants in the presence of NH_3. The basic trends in the data are fit quite well, although the quantitative agreement is not as good as might be desired. There are a number of possible sources of the deviations. First, there is the simplified treatment of the distribution function for the dimer. Second, we assume that solvated and free HO_2 have the same absorption cross section. A change in cross section could be significant since at 299 K as much as 30% of the HO_2 is bound by NH_3; this decreases to a maximum of 7% at 373 K. There is the possibility of systematic differences between the data of Lii et al. and Kircher and Sander due to different collision efficiencies of H_2 and N_2 or to the absorption cross sections used for HO_2. Finally, we note that at higher NH_3 concentrations we have reached 70% of the high-pressure limit. Since k_∞ is based on low-pressure data, this could introduce significant errors. We have not attempted to include corrections for these factors in our model; they would only result in an excess of adjustable parameters.

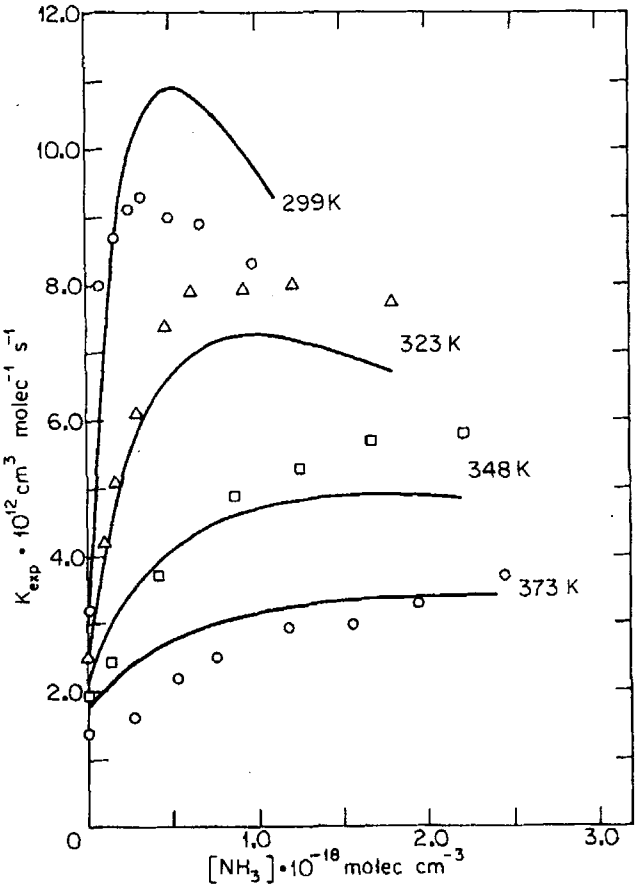

Figure 7. Calculated (solid lines) and experimental [10] (points) rate constants for self-reaction of HO_2 in the presence of NH_3.

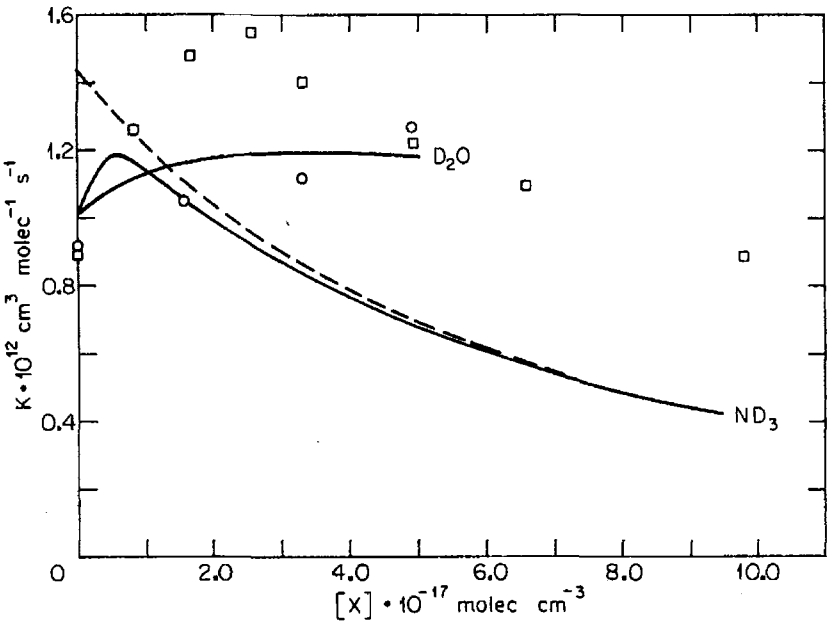

Figure 8. Calculated (—) and experimental [9] values of the rate constant for self-reaction of DO_2 as a function of concentration of D_2O (0) and ND_3 (□). Also shown is the high-pressure limit in the presence of ND_3 (- - -).

In Figure 8 we show the effect of D_2O and ND_3 on the rate constant for the self-reaction of DO_2 at 298 K [9]. For these calculations, k_6 was unchanged and V_5 was increased by 0.4 kcal mol^{-1}.The results for the D_2O effect agree reasonably well with experiment. However, the calculated rate constant in ND_3 is off by a factor of 2 at high concentrations. These data are in the high-pressure limit. As such they represent extreme extrapolations from the low-pressure data used to set the values of the parameters. The discrepancy between the calculated and experimental values represents a cumulative error of about 0.4 kcal mol^{-1} in the values of V_1, V_5, and the zero-point energy changes. Because of the many uncertainties in the data, mentioned above in respect to Figures 6 and 7, we have not attempted to carry out this fine tuning of the parameters.

VI. Summary

The pressure and temperature dependence of the self-reaction of HO_2 and DO_2 can be explained by assuming that the reaction proceeds via a cyclic, hydrogen-bonded dimer. Because of the large negative value (−4.9 kcal mol^{-1}) of the threshold energy for dissociation to products, the rate constants are relatively insensitive to this parameter. As a result, the observed isotope effect requires that zero-point energy changes must be much smaller in the transition state than in the reactants. These zero-point energy changes may be achieved by assuming a symmetrical transition state in which all

frequencies associated with hydrogen motions are fairly low ($\leq$1000 cm^{-1}). The third-order rate constant for the formation of the stabilized dimer is about the same for HO_2 and DO_2. The weaker pressure dependence of the self-reaction of DO_2 is due to the approach to the high-pressure limit. At low temperatures, the low-pressure limiting rate constant calculated for DO_2 is much smaller than that obtained by extrapolating the data of Kircher and Sander [2].

In order to reproduce the observed pressure dependences we must either assume very low collision efficiencies (0.035 for N_2) or have a less strongly bound dimer. If the collision efficiencies are very low, we have the possibility that the H_2O and NH_3 effects are due to their acting as efficient collision partners. The greater efficiency could be due to strong dipole-dipole interactions or the formation of hydrogen bonds with the open form of the dimer. However, with this mechanism it does not appear to be possible to explain the large negative temperature dependencies of the H_2O and NH_3 enhancements.

The rate enhancement by water vapor or ammonia may be explained by the formation of a hydrogen-bonded adduct, followed by displacement by HO_2 to form the stabilized dimer. In addition to dissociation to products, the dimer may undergo either back reaction to adduct or collisional dissociation to HO_2. These latter reactions are significant, especially in the presence of ammonia.

Since the threshold energy for dissociation of excited dimer to products is negative, the low-pressure rate constant is much less sensitive to this parameter than is the high-pressure limit. Consequently, measurements in the high-pressure limit would be desirable. For the DO_2 self-reaction this would require pressures of a few atmospheres. The addition of ND_3 will lower the required pressure.

In the absence of a polar collision partner, the high-pressure limit for HO_2 self-reaction will be reached only at prohibitively high pressures. However, a few hundred torr of NH_3 should be sufficient to reach this limit as long as the total pressure is sufficient for unimolecular decomposition of the dimer to be in the high-pressure limit. If the concentration of ammonia is high enough to bind most of the HO_2, it should be possible to test several of the assumptions made in this model. First, the decrease in rate constant with increasing ammonia concentration will provide a fairly direct measurement of the equilibrium constant for adduct formation. Also, measurements of the absorption cross section will determine the validity of the assumption that the cross section is the same for both bound and free HO_2. Finally, if enough HO_2 is bound it should be possible to determine if the adduct undergoes self-reaction.

How might it be possible to distinguish between the cyclic model of $(HO_2)_2$ considered here and the tetraoxide model considered by Patrick, Barker, and Golden [11]? With a suitable choice of

parameters the tetraoxide model can reproduce almost all of the results obtained here. The principle exception would be the isotope effect. This requires that, in the transition state, all hydrogen frequencies must be very low. Sufficiently low frequencies can be obtained with the cyclic model but not with the tetraoxide model.

As discussed in Section I, if the $HO_2 \cdot H_2O$ (or $HO_2 \cdot NH_3$) complex has the structure shown in Figure 3(a), then we expect that the water vapor effect in reactions in which HO_2 is attacked at the O atom would be weaker than for attack at the H atom. In this case, the strong H_2O effect observed for HO_2 self-reaction argues in favor of the cyclic intermediate. More experiments on the effects of polar species on reactions of HO_2 are needed. If the adduct has structure 3(b), then the tetraoxide model would not predict inhibition of reaction at large NH_3 concentrations. Although existing NH_3 data support inhibition, experiments at higher concentrations are needed.

A third possible means of testing the models would be to determine the electronic state of the product O_2. The tetraoxide model predicts that singlet O_2 would be formed; from the cyclic intermediate we expect to get triplet O_2.

Acknowledgments

We wish to thank Dr. John J. Lamb for helpful discussions during this work. This work was supported by the National Science Foundation and the Army Research Office under Grants Nos. CHE-79-26623 and DAAG-82-K-0043.

Bibliography

[1] R. A. Cox and J. P. Burrows, *J. Phys. Chem.*, **83,** 2560 (1979).
[2] C. C. Kircher and S. P. Sander, *J. Phys. Chem.*, **88,** 2082 (1984).
[3] B. A. Thrush and G. S. Tyndall, *Chem. Phys. Lett.*, **92,** 232 (1982).
[4] R. Patrick and M. J. Pilling, *Chem. Phys. Lett.*, **91,** 343 (1982).
[5] R-R. Lii, R. A. Gorse, M. C. Sauer, and S. Gordon, *J. Phys. Chem.*, **83,** 1803 (1979).
[6] R. Simonaitis and J. Heicklein, *J. Phys. Chem.*, **86,** 3416 (1982).
[7] S. P. Sander, M. Peterson, R. T. Watson, and R. Patrick, *J. Phys. Chem.*, **86,** 1236 (1982).
[8] R-R. Lii, M. C. Sauer, and S. Gordon, *J. Phys. Chem.*, **85,** 2833 (1981).
[9] E. J. Hamilton and R-R. Lii, *Int. J. Chem. Kinet.*, **9,** 875 (1977).
[10] R-R. Lii, R. A. Gorse, M. C. Sauer, and S. Gordon, *J. Phys. Chem.*, **84,** 813 (1980).
[11] R. Patrick, J. R. Barker, and D. M. Golden, *J. Phys. Chem.*, **88,** 128 (1984).
[12] P. A. Giguerre, *J. Phys. Chem.*, **85,** 3733 (1981).
[13] M. Mozurkewich and S. W. Benson, *J. Phys. Chem.*, **88,** 6429 (1984).
[14] H. Niki, P. D. Maker, C. M. Savage, and L. P. Breitenbach, *Chem. Phys. Lett.*, **73,** 43 (1980).
[15] We would also expect methanol to form a complex with HO_2. Although methanol is present in some of the reaction systems used in studies of HO_2 self-reaction, the concentration is small enough that it should not affect the rates.

[16] E.J. Hamilton and C.A. Naleway, *J. Phys. Chem.*, **80**, 2037 (1976).
[17] S.P. Sander and M.E. Peterson, *J. Phys. Chem.*, **88**, 1566 (1984).
[18] P.S. Nangia and S.W. Benson, *J. Phys. Chem.*, **83**, 1138 (1979).
[19] G. Fitzgerald and H.F. Schaefer, *J. Chem. Phys.*, **81**, 362 (1984).
[20] J.J. Lamb, M. Mozurkewich, and S.W. Benson, *J. Phys. Chem.*, **88**, 6435 (1984).
[21] M. Diem, T-L. Tso, and E.K.C. Lee, *J. Chem. Phys.*, **76**, 6452 (1982).
[22] R.J. Jakobsen, Y. Mikawa, and J.W. Brasch, *Spectrochim. Acta*, **23A**, 2199 (1967).
[23] S.W. Benson, "Thermochemical Kinetics," 2nd ed., Wiley, New York, 1976.
[24] E.B. Wilson, J.C. Decius, and P.C. Cross, "Molecular Vibrations," McGraw-Hill, New York, 1955.
[25] S.C. Chan, B.S. Rabinovitch, J.T. Bryant, L.D. Spicer, T. Fujimoto, Y.N. Lin, and S.P. Pavlou, *J. Phys. Chem.*, **74**, 3160 (1970).
[26] J. Troe, *J. Phys. Chem.*, **83**, 144 (1979).
[27] I.E. Klein and B.S. Rabinovitch, *Chem. Phys.*, **35**, 439 (1978).
[28] J-R. Cao and M.H. Back, *J. Phys. Chem.*, **88**, 3074 (1984).